A thermodynamic study of ferrocene modified hairpin oligonucleotides upon duplex formation: applications to the electrochemical detection of DNA†

Grégory Chatelain,[a] Hugues Brisset[b] and Carole Chaix*[c]

Received (in Montpellier, France) 1st October 2008, Accepted 22nd January 2009
First published as an Advance Article on the web 26th February 2009
DOI: 10.1039/b817057f

New electrochemical probes are being developed for nucleic acid detection. A ferrocenyl phosphoramidite synthon (Fc) is synthesized and then incorporated into stem-loop structured oligodeoxyribonucleotides (ODNs) by automated solid-phase DNA synthesis. The thermodynamic study shows slight destabilization of the structures obtained due to the presence of ferrocene moieties (ΔG°_{298} = −1.28 to −1.82 kcal mol^{-1} for hairpin folding and ΔG°_{298} = −14.66 to −17.16 kcal mol^{-1} for duplex) compared to the unmodified sequence (ΔG°_{298} = −2.04 kcal mol^{-1} for hairpin folding and ΔG°_{298} = −18.97 kcal mol^{-1} for duplex). When spotting these ferrocenyl stem-loop structured ODNs on a gold electrode microarray, a self-structuring of the probes occurs on the electrode surface. The hairpin opening, generated by the hybridization with the complementary nucleic acid target, induces variations in both current intensity and potential of the ferrocenyl electrochemical signal by cyclic voltammetry (CV). The effects of the number of ferrocenes in the hairpin sequences on thermodynamic stability and the electrochemical response of the probes upon DNA target hybridization are studied. These ferrocene modified stem-loop ODNs allow complementary target detection by cyclic voltammetry.

Introduction

The highly specific recognition property of DNA strands is of great interest in the development of efficient and easy to handle tools for molecular biology. This interaction is now traditionally used as a generic tool in biological techniques and plays a crucial role in a broad range of applications, including clinical diagnosis,[1] environmental monitoring, forensic analysis and bio-terrorism. The growing interest of chip-based characterization of gene expression patterns and pathogen detection is an illustration of the high potential of DNA technologies. Strong demand is currently emerging to develop sensitive and labelless systems allowing real-time monitoring. In this field, the molecular beacon strategy has attracted significant interest. This solution-phase optical method has proved to be highly specific in complex biological samples and is also suitable for multidetection biochip devices. A molecular beacon is a dual-labelled oligonucleotide probe that fluoresces upon hybridization with a complementary target.[2–7] The oligonucleotide is modified at one end with a fluorescence reporter dye and at the opposite end with a fluorescence quencher. The molecular beacon is designed to form a stem-loop structure in the absence of the target, forcing the fluorescence reporter group closer to the quencher group. In this conformation, fluorescence is quenched. In the presence of the complementary target molecule, the molecular beacon opens due to the preferential formation of the more stable probe–target duplex, increasing the distance between the reporter and the quencher, and restoring fluorescence. In the literature, the thermodynamic stability of hairpins[8,9] and molecular beacons[10,11] has been largely studied. The competition between hairpin and duplex formations improves the binding specificity compared with linear probes. The unique target recognition and signal transduction capabilities of molecular beacons have led to their use in many biochemical and biological assays including NASBA,[12] quantitative PCR,[13–15] real-time monitoring DNA methylation[16] and DNA–protein interactions.[17] In a general manner, the molecular beacon strategy appears to be very specific but not really sensitive, as a detection limit of 0.1 μM DNA target is generally reached by methods using molecular beacons in solution[6] and 50 pM is currently detected on biochips which require a preliminary immobilization of molecular beacons on a support before DNA target detection.[18]

Electrochemical detection is a method of choice for biosensor development as this technique is versatile, relatively simple to instrument and as sensitive as fluorescence. We focus here on the development of redox oligonucleotide probes capable of detecting DNA targets directly in a small volume of sample (10 μL) without labelling. As for the molecular

[a] *UMR 5180-CNRS, Lab. des Sciences Analytiques Université Lyon, UCBL Bât. CPE, 43 Bd du 11 Nov. 1918, 69622, Villeurbanne Cedex, France. E-mail: gregory.chatelain@cpe.fr; Fax: 33 (0)4 72 44 84 79; Tel: 33 (0)4 72 43 14 13*
[b] *Centre Interdisciplinaire de Nanoscience de Marseille, CINaM-UPR 3118 Université Aix Marseille, Campus Luminy Case 913, 13288, Marseille Cedex 09, France. E-mail: hugues.brisset@univmed.fr; Fax: 33 (0)4 91 82 95 80; Tel: 33 (0)4 91 82 95 87*
[c] *UMR 5180-CNRS, Lab. des Sciences Analytiques Université Lyon, UCBL Bât. CPE, 43 Bd du 11 Nov. 1918, 69622, Villeurbanne Cedex, France. E-mail: carole.chaix-bauvais@univ-lyon1.fr; Fax: 33 (0)4 72 44 84 79; Tel: 33 (0)4 72 44 83 06*
† Electronic supplementary information (ESI) available: MALDI-TOF masses and HPLC analyses of the hairpins A–F. See DOI: 10.1039/b817057f

beacon strategy, stem-loop structures are investigated to provide a detectable change in the probe response upon hybridization.

In the literature, the elaboration of electrochemical "molecular beacons" has already been described. Stem-loop structured oligonucleotides are functionalized at one extremity with various redox centers such as ferrocene,[19–21] methylene blue[22–24] or thionine.[25] A thiol arm is generally introduced at the other end, allowing probe immobilization on a gold surface. The hairpin opening during hybridization induces a significant variation in the system's electrochemical signal. These methods are relatively sensitive (target detection limit of 10 pM) but not efficient enough to be able to detect targets without amplification.

Ferrocene (Fc) is the most commonly employed label in electrochemical DNA biosensors and microarrays due to its good stability and easy chemistry to handle.[26] In previous papers, we reported a method to introduce ferrocene moieties in oligonucleotide sequences *via* automated synthesis.[27–30] The resulting redox molecule affords a very sharp electrochemical response, in a potential range compatible with the use of biomolecules ($E_{ox} \sim 200$ mV *vs.* gold electrode as reference). Furthermore, the high sensitivity of ferrocene to its electronic and steric environment is of interest to DNA electrochemical detection.

In a recent work, we introduced ferrocene moieties between the stem and loop of a DNA hairpin structure and we demonstrated that modification of the Fc environment upon hybridization could be observed by cyclic voltammetry.[31]

Here, we describe the thermodynamic study of two different designs of Fc-modified hairpin oligodeoxynucleotides (Fc-ODNs), *i.e.* the first corresponding to the hairpin with Fc incorporated between the stem and loop; the second referring to Fc incorporations at each end of the sequence. Thermodynamic parameters of both closed and opened structures are investigated. The influence of the number of Fc and their position in the hairpin on the equilibrium between the two conformations, folded hairpin and duplex, are evaluated. This study allows us to determine the participation of Fc in the stability of both states.

Finally, the most promising structures selected from the thermodynamic data interpretation are evaluated as sensitive probes for the electrochemical detection of DNA targets. The preliminary results on test specificity are presented here. We confirm that the sensitivity limit achieved by this method, where both the Fc-modified hairpin and the DNA target are in solution, can be efficiently improved by the use of a hairpin modified by eight Fc in the loop.

Results and discussion

Fc-ODNs were synthesized according to the method described in a previous paper.[27] The bifunctional ferrocene phosphoramidite (1-[3-*O*-dimethoxytritylpropyl]-1′-[3′-*O*-(2-cyanoethyl-*N*,*N*-diisopropylphosphoramidityl)propyl] ferrocene) was first synthesized from the Fc bis-propanol provided by Ezus (Villeurbanne, France) in two steps. This synthon was used in the synthesizer to incorporate Fc in ODN sequences directly during solid-phase synthesis. After optimization, the Fc synthon coupling yield obtained from HPLC analyses of crude hairpin syntheses was 97%. The A, T, C and G synthons typically reacted with an average coupling yield of 98%, measured by DMT quantification.

Oligonucleotide design

Fig. 1 shows the general structure of the six hairpin ODNs investigated in the study. The stem-loop sequence corresponds to a beacon structure developed by bioMérieux for influenza RT-PCR analysis. The oligonucleotide is designed to fold into a hairpin structure formed with a loop of twenty bases and a short stem of six Watson–Crick paired bases. Fc modifications were localized either at both hairpin ends, like a traditional beacon, or between the stem and loop (Fig. 1). The number of Fc incorporated in the ODN sequence varies from two to eight, in order to examine their influence on both thermodynamic parameters and the electrochemical response of the resulting probes.

Melting temperature analysis

We used the UV melting curve analysis method to calculate the melting temperature (T_m) values of folded hairpins and hairpin/target duplexes. This method necessitates to calculate first the fraction of the single strand under hairpin state and duplex state at each temperature ($\alpha(T)$) from the UV melting curves. The complete method is described in the Experimental section. Data are summarized in Table 1.

When compared with the T_m of the unmodified sequence, the data show that two and four Fc incorporations between the hairpin's stem and loop slightly decreased the resulting T_m (−3.9 °C for hairpin A and −1.5 °C for hairpin B) while six and eight Fc modifications allowed to cancel out this negative effect (+0.2 °C for hairpin C and +0.5 °C for hairpin D) (Table 1, left). These results indicate that the incorporation of few Fc (up to four) between the stem and loop adds some strain in the loop, discouraging hairpin folding, whereas further Fc additions (six and eight) restabilize the hairpin structure by adding more flexibility in the chain.

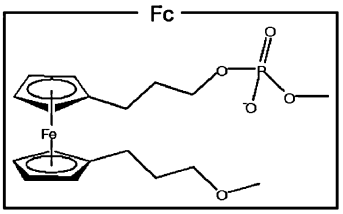

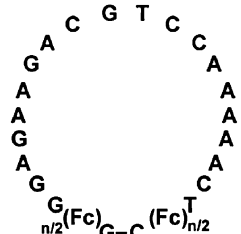

Hairpin	Modifications		
	n	m	i
unmodified	0	0	0
A	2	0	0
B	4	0	0
C	6	0	0
D	8	0	0
E	0	2	1
F	0	4	1

Fig. 1 Structure of the ferrocene (Fc) incorporated in the ODN sequences (top left) and general design of the stem-loop Fc oligonucleotides (Fc-ODNs).

Table 1 Values of T_m of folded hairpins and hairpin-target duplexes

	Folded hairpin		Hairpin/complementary target duplex	
Hairpin	T_m/°C	ΔT_m/°C	T_m/°C	ΔT_m/°C
Unmodified	50.0 (0.9)		64.8 (0.8)	
A	46.1 (0.5)	−3.9	63.4 (0.7)	−1.4
B	48.5 (0.9)	−1.5	61.6 (0.6)	−3.2
C	50.2 (0.6)	+0.2	60.5 (0.3)	−4.3
D	50.5 (0.6)	+0.5	61.0 (0.6)	−3.8
E	52.0 (0.9)	+2.0	64.2 (0.2)	−0.6
F	50.6 (0.1)	+0.6	62.0 (0.8)	−2.8

T_m values are obtained from graph $\alpha = f(T)$ and correspond to $\alpha = 0.5$. Data are the mean values of minimum three experiments with standard deviations in parentheses. Complementary target: 5′TTTTTAGTTTTTGGACGTCTTCTCCTTTTT-3′

When the Fc modifications were placed at the end of the stem, the structure appeared to be more stable than the unmodified structure. But considering the standard deviation of the T_m values (±0.9 °C), this variation was not significant enough to be considered.

Fig. 2 shows the α values of hairpin/target duplexes *vs.* temperature (T) (see Experimental section). The curves show that the transitions with modified hairpins occurred over a larger range of temperature than with the unmodified sequences. These broad transitions indicate a loss of system cooperativity generally associated with a decrease in specificity.[32] The T_m values of hairpin/target duplexes correspond to the temperature at $\alpha = 0.5$ and are indicated in Table 1. Hairpin E has a negligible effect on duplex stability as its T_m variation (−0.6 °C) is included in the whole standard deviation of the measure (0.9 °C). The other data reveal that an increase in the number of Fc slightly destabilizes the duplex, regardless of their position in the structure (either between the stem and loop (from A to D) or at the end of the sequence (from E to F)). The worst thermal destabilization was observed for hairpin C ($\Delta T_m = -4.3$ °C). In a general manner, Fc modifications at the hairpin extremities were less destabilizing than between the stem and loop, in hairpins with the same number of modifications in the sequence.

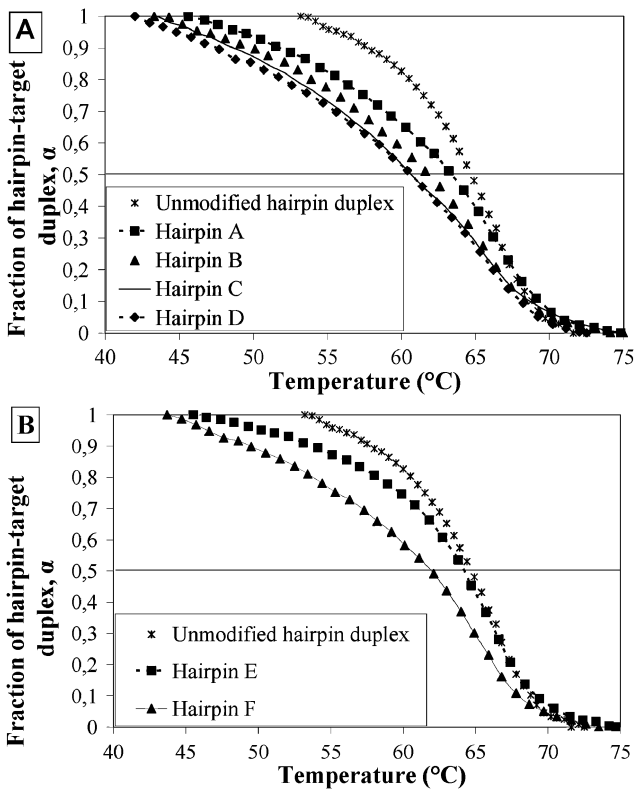

Fig. 2 Values of α *vs.* temperature calculated from UV melting curves of the hairpin/target duplexes compared to the unmodified hairpin duplex: (A) hairpins A–D, (B) hairpins E and F; T_m values were obtained for $\alpha = 0.5$ (solid line).

Thermodynamic study of the Fc-modified hairpins

The enthalpy, entropy and free energy changes involved in duplex formation from the hairpin structures were studied. Thermodynamic parameters were calculated from the $\alpha(T)$ values using the equations reported in the Experimental section. The parameters obtained from the individual melting curves are shown in Table 2.

The enthalpy change ΔH° and entropy change ΔS°, which both describe the equilibrium state between unfolded and folded molecules, were determined using van't Hoff plot (eqn (4) in the Experimental section). The ΔG° values reflect the energetics barriers of the different conformations in an equilibrium state at 25 °C. The lower the ΔG° value, the higher the energetics barrier has to be to induce a conformational change in the structure. The ΔG° values describe the stability of the nucleic acid structures.

Considering thermodynamic parameters, Fc-modified hairpins were less stable than the unmodified hairpin. Nevertheless, the calculated free energy ΔG° decreased when the number of Fc-modifications increased at the stem-loop intersection (from −1.28 kcal mol^{-1} for two Fc to −1.81 kcal mol^{-1} for eight Fc), tending towards the value of the unmodified hairpin ($\Delta G^\circ_{298} = -2.04$ kcal mol^{-1}). The same trend was observed for the variations of ΔH° and $T\Delta S^\circ$. These results are in agreement with the T_m values of Table 1, which revealed that the hairpins could be stabilized by incorporating a higher number of Fc in the loop. In the literature, Williams *et al.*[33] introduced ethylene glycol moieties between the stem and the loop. They showed that these modifications considerably destabilized the hairpin structure and that destabilization was even greater with a higher number of spacers. In our case, Fc modifications destabilized the stem-loop structure when the number was relatively low but this destabilization diminished when the Fc number increased, probably because of a larger loop size resulting from Fc incorporations (when $n = 6$ or 8). This helped to overcome the initial rigidity on the loop caused by the inflexible biofunctional Fc moieties (when $n = 2$ or 4).

In the case of hairpins with Fc positioned at the stem extremities, an increase of the ΔG°_{298} values was observed, related to a slight destabilization of the structure, but the increase in the number of Fc in this region did not significantly modify the ΔG°_{298} of the structure (−1.82 and −1.76 kcal mol^{-1} for two and four Fc, respectively).

The ΔG°_{298} calculation of hairpin-target duplexes showed a notable destabilization when Fc were close to the double

Table 2 Thermodynamic parameters of hairpin and hairpin/target duplex formations

	Folded hairpin			Hairpin/complementary target duplex		
Hairpin	ΔH°/kcal mol^{-1}	$T\Delta S^\circ$/kcal mol^{-1}	ΔG°_{298}/kcal mol^{-1}	ΔH°/kcal mol^{-1}	$T\Delta S^\circ$/kcal mol^{-1}	ΔG°_{298}/kcal mol^{-1}
Unmodified	−26.82 (1.32)	−24.73 (1.19)	−2.04 (0.14)	−86.48 (6.33)	−67.65 (5.66)	−18.97 (0.77)
A	−20.15 (1.15)	−18.77 (0.89)	−1.28 (0.14)	−75.83 (2.28)	−58.71 (2.09)	−17.16 (0.22)
B	−21.54 (1.82)	−19.97 (1.79)	−1.59 (0.20)	−67.27 (2.71)	−51.26 (2.38)	−15.93 (0.29)
C	−23.98 (2.13)	−22.35 (2.09)	−1.70 (0.11)	−63.44 (5.25)	−47.98 (4.77)	−15.31 (0.57)
D	−23.31 (1.79)	−21.46 (1.79)	−1.81 (0.11)	−57.00 (3.62)	−42.32 (3.28)	−14.66 (0.42)
E	−22.59 (1.86)	−20.77 (1.79)	−1.82 (0.05)	−75.85 (1.06)	−59.30 (1.49)	−16.61 (0.70)
F	−22.72 (1.88)	−20.95 (1.79)	−1.76 (0.12)	−73.17 (5.77)	−56.62 (5.07)	−16.64 (0.70)

ΔH° and ΔS° were evaluated from the graph $\ln(K(T)) = f(1/T)$ according to eqn (4). ΔG° was calculated from eqn (5). Data are the mean values of minimum three experiments with standard deviations in parentheses.

strand helix. This destabilization was stronger with a higher number of Fc (ΔG°_{298} = −17.16 and −14.66 kcal mol^{-1} for hairpin A and D, respectively, compared to −18.97 kcal mol^{-1} for unmodified hairpins). Fc modifications destabilized the duplex whatever their position in the hairpin sequence. Nevertheless, Fc positioned at hairpin extremities were less destabilizing (ΔG°_{298} = −16.61 and −16.64 kcal mol^{-1} for hairpin E and hairpin F, respectively). Globally, these results correlate with the previous interpretations of α plots and T_m values (Table 1).

Thermal and thermodynamic studies tend to prove that Fc incorporation in the hairpin sequence slightly destabilizes both self-folded and double-strand conformations. This destabilization is more distinguishable when Fc are incorporated between the stem and loop. Surprisingly, the duplex structure suffers the greatest destabilization. A schematic view of Fc impact on hairpin and duplex equilibria is shown in Fig. 3, comparing the thermodynamic stability of the four Fc modified hairpins, B and F.

Electrochemical detection

Ferrocenes bound to oligonucleotides act as electrochemical markers, affording a sharp chemical response which is highly sensitive to ionic and steric surrounding media. In the literature, Fc modified stem-loop structures have already been described as efficient probes for DNA electrochemical detection after anchoring onto electrode surfaces.[19–21] By comparison with published works in this field, the main advantage of our strategy lies in the incorporation of numerous ferrocenes in the ODN probes to enhance the system's electrochemical response.

With a view to correlating the thermodynamic features of Fc-hairpins with their electrochemical response on electrode network microarrays, the electrochemical signal of the probes was studied by cyclic voltammetry (CV). The experiment was performed with Fc-modified hairpins B, D and F, on a gold electrode microarray developed by bioMérieux (Fig. 4). This is a multiplot plastic-based chip specially designed for a low cost, low density biodevice.[34] In this work, we addressed and further recorded the response of the eight plots simultaneously, by CV. A droplet (10 μL) of each Fc-hairpin was deposited on the working area to achieve electrochemical measurements.

CV of the two hairpin designs (hairpins B and D with four and eight modifications between the stem and loop, respectively, and hairpin F with four modifications at the end of the stem) showed that the hairpins did not respond equally (Fig. 5). A very intense signal was recorded with hairpin F compared to hairpin B, revealing the influence of the Fc positions on the electrochemical response. Indeed, for hairpin B, the Fc were placed inside the structure while for hairpin F, the Fc were outside the structure, suffering less strain from the

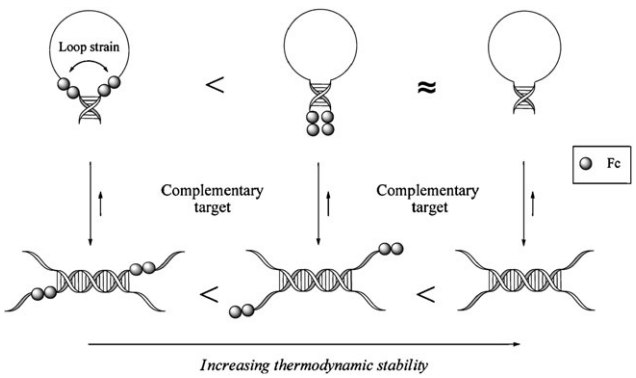

Fig. 3 Thermodynamic stability comparison between the four Fc-modified ODNs (B and F) and the unmodified hairpin, in relation to hairpin and duplex formation.

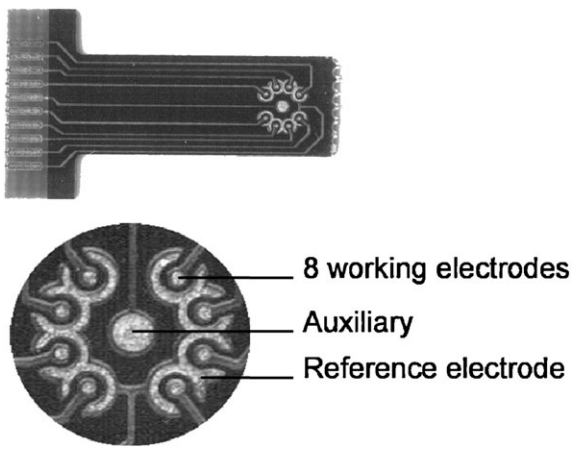

Fig. 4 Gold electrode microarray (length = 25 mm, width = 7 mm and thickness = 0.5 mm, with embedded electrical circuits and back contacts) and details of the working area covered by the 10 μL droplet; Working electrode surface: 3.1 × 10^{-4} cm^2; reference gold electrode surface: 1.092 × 10^{-2} cm^2; auxiliary gold counter electrode surface: 2.82 × 10^{-3} cm^2.

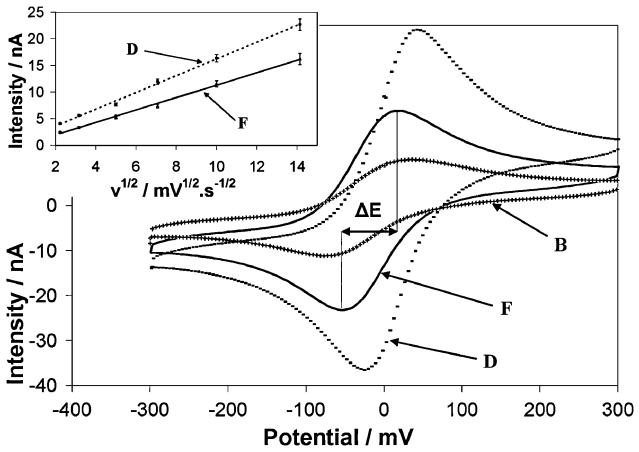

Fig. 5 Electrochemical response of hairpin B (four Fc-modifications between the stem and loop), hairpin D (eight Fc-modifications between the stem and loop) and hairpin F (four Fc modifications at the end of the stem) by cyclic voltammetry, at 80 min after the deposition of probe solution (50 μM) on the gold electrode microarray (scan rate = 100 mV s^{-1}) and oxidative current variation (I_{ox}) as a function of the scan rate square root for hairpins D and F (top left, $I_{ox} = f(v^{1/2})$).

folded conformation. We assume that Fc positioning at the hairpin termini favors their proximity to the electrode surface when deposited on the microarray. The electron transfer between Fc groups is amplified inducing an increase in the electrochemical signal. By incorporating a higher number of ferrocenes in the loop (hairpin D), a significant increase of signal intensity was observed by CV. Current intensity at the oxidation peak of Fc (I_{ox}) was recorded at different scan rates (v), for hairpins D and F. A linear relationship was found with the scan rate square root ($v^{1/2}$) ($I_{ox} = 1.576v^{1/2} - 0.458$; $R^2 = 0.9974$ for hairpin D, and $I_{ox} = 1.171v^{1/2} - 0.340$; $R^2 = 0.9947$ for hairpin F) (Fig. 5, top left) and not with v, indicating that no adsorption phenomena of Fc-ODNs occurred on the microarray surface in these experimental conditions.[35] The same behavior was observed for hairpin B.

For each hairpin A–F, the charge transfer to the electrode associated with Fc oxidation (Q_{ox}) has been estimated (Fig. 6). In a first experiment, CV have been achieved with hairpin solutions at the same concentration (100 μM) (Fig. 6A). Then, Q_{ox} was calculated by integrating the anodic peak area of Fc on CV, as described by Farre *et al.*[36] The charge transfer to the electrode increases exponentially with the number of Fc in the sequence, for structures A–D. A single Fc moiety included in the sequence appears to be less available for redox reaction than a Fc surrounded by other Fc. Different Q_{ox} were also observed for E and F which confirm that the individual Fc response is not equivalent in the different probes. In a second experiment, the charge transfer to the electrode was also calculated for the different probes, at a constant concentration of ferrocene in solution (200 μM) (Fig. 6B). In these conditions, hairpin concentrations in solution ranged from 25 μM (for $n = 8$) to 100 μM (for $n = 2$). A linear increase of Q_{ox} was observed for hairpins A–D confirming that, for one ferrocene moiety, the charge transfer to the electrode is different when the molecule is included in the hairpins A–D. We can hypothesize that there is an effect on the signal intensity

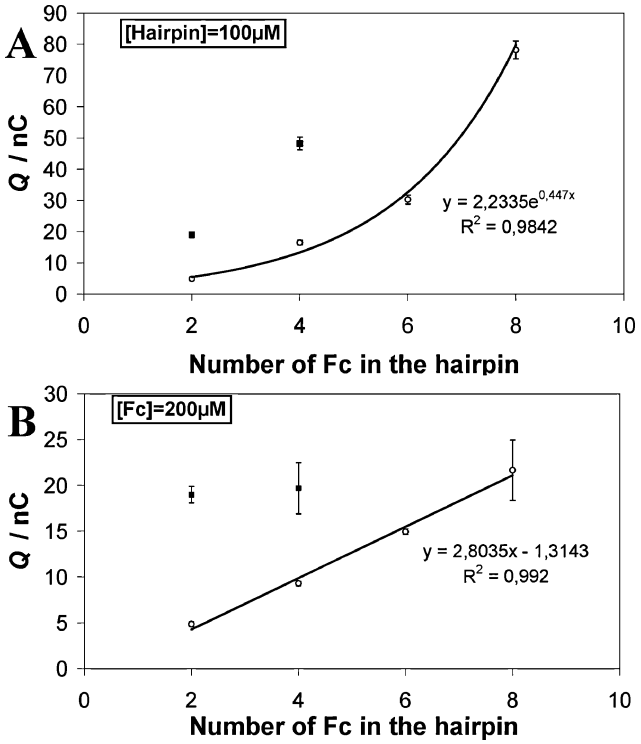

Fig. 6 Evolution of the charge transfer (Q/nC) *vs.* the number of Fc; Q is calculated by integrating the current intensity peak area of Fc's oxidative wave from CV analysis; (A) at a constant concentration of probes, [hairpin] = 100 μM; (B) at a constant concentration of ferrocenes, [Fc] = 200 μM; measured at 80 min after deposition of 10 μL droplet on the gold electrode; hairpins E and F (■), hairpins A–D (○).

induced by an increasing number of Fc between the stem and loop of the sequence. On the other hand, hairpins E and F exhibit the same charge transfer. In this latter design, ferrocenes positioned at the ends of hairpin undergo less strain from the oligonucleotidic sequence and are more available for redox reaction. The more intense response of hairpin D allows one to work with lower concentrations of probe in solution, diminishing the detection threshold of the system.

Then, we followed the electrochemical response of hairpins B, D and F after adding either the hairpin loop complementary or non-complementary sequence. Experiments were achieved with solutions of B and F at 100 μM. Hairpin D was used at 5 μM. After stabilization of the signal for 80 min, 5.5 equivalents of the target were introduced in the medium. Parameters I_{ox} and ΔE were recorded. As reported in a previous paper,[31] the binding reaction modified both I_{ox} and ΔE. A decrease in I_{ox} was observed over a short period of time and was ascribed to a temporary perturbation of the molecules close to the surface due to the hybridization reaction. The ΔE variation was much more reproducible and was ascribed to a real change of the Fc environment, resulting from the hybridization process. In this work, we followed the ΔE variation on the CV for hairpins B, D and F. In order to compare data from the eight working electrodes of the chip with data from separate chips, we normalized the measurements using eqn (1):

$$NE = (\Delta E - \Delta E_0)/\Delta E_0 \quad (1)$$

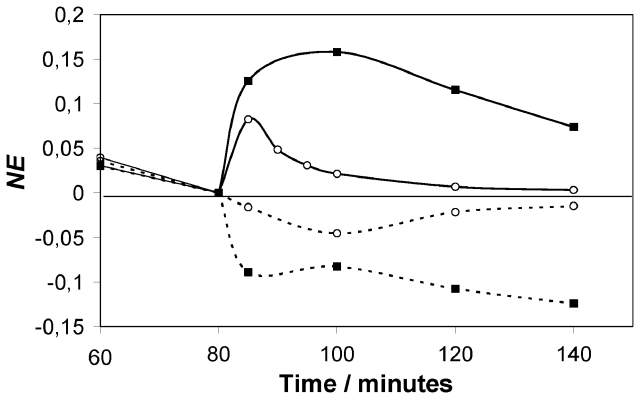

Fig. 7 Electrochemical response of Fc-modified hairpins B (■) and F (○) (four Fc modifications) during the hybridization reaction ($NE = (\Delta E - \Delta E_0)/\Delta E_0$ against time). Each test was performed with 100 μM probe solution and 5.5 equivalents of complementary target (solid line) or 5.5 equivalents of non-complementary target (dashed line). Targets were added 80 min after probe deposition on the microarray.

where *NE* is the normalized value of ΔE and ΔE_0 is the ΔE measurement just before target addition. Addition of the complementary target to the medium induced a positive variation. This behavior was ascribed to a morphological change of the hairpin structure adsorbed on the electrode resulting from duplex formation. The hybridization kinetics appeared to be rapid. ΔE started to decrease again after a reaction time of 20 min for B and after 5 min for D and F, probably due to reorganization of the (Fc-probe/target) duplexes on the surface. Conversely, the addition of the non-complementary target slightly decreased ΔE probably due to an electrostatic effect of the negatively charged target on probes that reduce the *NE*. This side effect disappeared under the strong positive variation of *NE* resulting from hybridization on adding the complementary target (Fig. 7). The response was significant, reproducible and specific. In conclusion, we confirmed that ΔE is a good parameter to follow the hybridization reaction.

To compare the signal variation of both hairpins B, D and F, we recorded *NE* at 5 min after the addition of 5.5 equivalents of the target (Fig. 8). At this time, a plateau was reached for the *NE* value with hairpin B, indicating that the hybridization reaction was complete. It was also the most significant

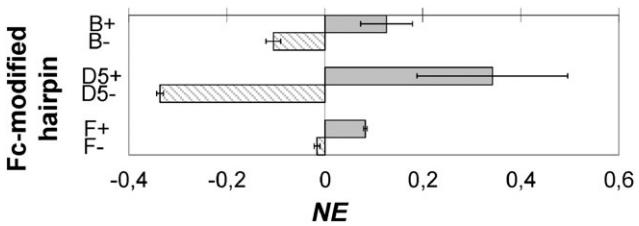

Fig. 8 Hybridization tests with Fc-ODNs B, D and F. Tests with hairpins B and F were performed with 100 μM probe solutions and test with hairpin D was performed with 5 μM probe solution (D5). 5.5 equivalents of the complementary target (grey, +ve) or 5.5 equivalents of the non-complementary target (black hatching, −ve) were introduced in the solution at t_0. *NE* values were calculated at 5 min after target addition. The histogram shows the mean values from three experiments.

time to discriminate between the positive and negative responses with the hairpins. Hybridization tests were achieved under the same conditions for both complementary and non-complementary sequences. The values presented are the mean values from three experiments.

The data show that the more stable hairpin in terms of thermodynamic parameters (hairpin F, Tables 1 and 2) provides the lowest electrochemical signal variation during the hybridization test. *NE* variation was much more significant for hairpins B and D. This result confirms our assumption that the greater strain that exists on the Fc in the folded hairpin B is associated with an electrochemical signal variation of higher amplitude when it opens for hybridization. But one drawback of the use of hairpin B was its low electrochemical signal that required working with a high probe concentration in solution (100 μM). By using hairpin D, we succeeded in achieving the hybridization test with a much lower concentration of probe. Indeed, a 5 μM solution of D was sufficient to efficiently detect the Fc redox signal. This interesting result also confirms our hypothesis that a higher number of Fc in the loop provides a greater electrochemical signal that permits to decrease the detection limit. We estimate that the sensitivity reached by our system is currently around 1 μM, by the use of D as electrochemical probe. This sensitivity is of the same order of magnitude as that reached by the system of Luo *et al.*[37] The authors describe a similar immobilization-free sequence electrochemical detection of DNA, by the use of ferrocene modified peptide nucleic acids (PNA) as probes. They claim a linear detection range between 0.25 and 2 μM on a bare ITO working electrode microsystem. In our case, we assume that the detection limit could be improved further by incorporating a higher number of Fc in the probe sequence which would allow to work at lower concentrations of probe in solution. Furthermore, probe immobilization on the electrode device should greatly improve the sensitivity of our system. In this latter case, we expect to reach a better sensitivity than that claimed by Heeger *et al*[19,20] using a single-ferrocene modified hairpin system.

Conclusions

The modification of ODN hairpin structures by ferrocenes during automated DNA solid-phase synthesis has proved to be a good method for the easy incorporation of numerous electrochemical markers in the sequence. The positions of the Fc inside the sequence, between the stem and loop or at the stem extremities, have a moderate impact on the thermodynamic stability of the resulting self-folded hairpin and hairpin–target duplex conformations. It is worth noting that it is the duplex structure that is the most destabilized by Fc modifications. We can also conclude that the presence of Fc has no consequence on the specific opening of the structure for binding with the complementary target. This property has been successfully used to develop a diagnostic test by electrochemistry. The comparison of the two hairpin designs B and F with the same number of modifications in the sequence shows a better response from the hairpin bearing Fc between the stem and loop (hairpin B). We also confirm that a higher number of Fc in the loop provides a great improvement of the detection

limit of the microsystem. This immobilization-free DNA electrochemical detection method can be carried out in less than 10 min. Therefore, it has the potential to be developed into a powerful tool for sequence-specific DNA detection and quantification. The ultimate goal of this work is to address these structures on the surface of a gold electrode microarray to increase system sensitivity significantly and to enable the construction of a labelless multidetection biochip device.

Experimental

Chemicals

Ferrocene bis-propanol was purchased from EZUS (Villeurbanne, France). DNA synthesis reagents and solvents were purchased from Glen Research (Sterling, Virginia). The other chemicals such as electrochemical salts and solvents were purchased from Sigma-Aldrich (Saint Quentin Fallavier, France).

Fc phosphoramidite synthon synthesis

The 1-[3-*O*-dimethoxytritylpropyl]-1′-[3′-*O*-(2-cyanoethyl-*N*,*N*-diisopropylphosphoramidityl)propyl]ferrocene (Fig. 1) was synthesized in two steps from the ferrocene bis-propanol according to a protocol described in a previous paper.[27] After synthesis, the synthon was characterized by ^{31}P NMR, ^{1}H NMR and dried overnight under vacuum just before use. A solution of the Fc phosphoramidite synthon (0.13 M) in dry acetonitrile was used to incorporate ferrocene moieties in the oligonucleotide sequences during the automated synthesis.

Oligonucleotide synthesis

Fc-modified oligonucleotides (Fig. 1) were synthesized using standard phosphoramidite chemistry on an Applied Biosystems DNA synthesizer 394 (Foster City, USA). Hairpins were purified by HPLC using a DeltaPak C18 15 μm 300 Å with a gradient of solution A (0.05 M TEAAc, pH = 7) and solution B (0.05 M TEAAc–acetonitrile, 50 : 50). Oligonucleotide purity was controlled by HPLC using an X-terra MS C18 2.5 μm column. Analyses were achieved with a gradient (from 10% B to 100% B) in 40 min at 60 °C. Then, oligonucleotides were characterized by MALDI-TOF mass spectrometry on an Applied Biosystems Voyager DE-PRO (Foster city, USA), using 2′,4′,6′-trihydroxyacetophenone monohydrate (THAP) as matrix (ESI†)

Complementary target (CT: 5′-TTTTTAGTTTTTGGACG-TCTTCTCCTTTTT-3′), and non-complementary target (NCT: 5′-TTTTTATTGAGATTCCCGAGATTGATTTTT-3′), were purchased from Eurogentec (Angers, France).

Apparatus

Melting temperature measurements were performed on an Uvikon UV spectrophotometer XL from Secomam. UV cell temperature was controlled by a Bio-Tek Peltier thermosystem.

Electrochemical measurements on biochip were performed on the ApiT8 gold electrode device[34] kindly provided by bioMérieux (Marcy-l'Etoile, France). It contained eight sensing plots made of small area (3.1×10^{-4} cm^2 surface) working electrodes equally distributed in the circular section of the device, together with a central gold counter electrode (2.82×10^{-3} cm^2 surface) (Fig. 5). A common gold electrode reference (1.092×10^{-2} cm^2) was designed with individual rings placed around each working electrode and kept in contact one to each other. This system was connected to a Biologic multichannel potentiostat VMP2 (Biologic Science Instruments, Pont de Claix, France). Results were recorded with EC-Lab software from Biologic Science Instruments.

UV melting experiments

The molecular extinction coefficients (ε) of the unmodified hairpin sequences (i = 0, 1) were calculated from the standard equation reported by Cantor *et al.*[38] and Cavaluzzi *et al.*[39] that takes into account the nearest neighbour coefficients at 20 °C in the formula. The ε values of unmodified hairpins were 322 L mmol^{-1} cm^{-1} and 330.5 L mmol^{-1} cm^{-1} for i = 0 and 1, respectively (Fig. 1). We used the ε value of the ferrocene bis-propanol measured at 260 nm (ε_{Fc} = 3.5 L mmol^{-1} cm^{-1}), as reported in a previous work.[27] Thus, the molar extinction coefficients of modified ODNs were calculating by adding the adequate number of ferrocene ε_{Fc} values to the ε of the corresponding unmodified structure. For A to F sequences, the following molecular extinction coefficients were calculated: ε_A = 329.0 L mmol^{-1} cm^{-1}, ε_B = 336.0 L mmol^{-1} cm^{-1}, ε_C = 343.0 L mmol^{-1} cm^{-1}, ε_D = 350.0 L mmol^{-1} cm^{-1}, ε_E = 337.5 L mmol^{-1} cm^{-1}, ε_F = 344.5 L mmol^{-1} cm^{-1}.

Experiments on hairpin ODNs were achieved with ODN solutions (1 μM) in phosphate buffer (25 mM Na_2HPO_4, 25 mM KH_2PO_4, 250 mM NaCl, pH = 6.4). Experiments on hairpin/target ODNs were achieved with 1 μM of each ODN in the same buffer. The absorbance at 260 nm was continuously monitored over a temperature range from 90 to 10 °C. Specifically, the temperature was initially held at 90 °C for 5 min, and then decreased to 10 °C, at a rate of 0.5 °C min^{-1}. After 5 min stabilization at 10 °C, the temperature was then raised back to 90 °C (0.5 °C min^{-1}) for melting temperature measurements.

Thermodynamic parameter calculations

Dissociation constants ($K(T)$) were calculated for hairpin ODNs and hairpin/target duplexes as described by Marky *et al.*[40] and Durand *et al.*[41]

For this analysis, it is first necessary to cast raw optical data into the fraction of the single strand under hairpin state and duplex state at each temperature, $\alpha(T)$, for both hairpin folding and hairpin/target binding experiments, respectively. To accomplish this, upper and lower absorption baselines (A_U and A_L) were determined by calculating the absorbance derivative (dA/dT). A_U and A_L values corresponded to both dA/dT minimums of the curve. Next, the folded or bound fraction parameter $\alpha(T)$ was computed for each temperature (T) according to eqn (2):

$$\alpha(T) = (A_U - A(T))/(A_U - A_L) \quad (2)$$

where $A(T)$ is the absorbance at temperature T.

Consequently, a plot of $\alpha(T)$ *vs.* temperature was constructed and used to calculate the T_m value by interpolating

$\alpha = 0.5$. The transition equilibrium $K(T)$ was calculated at various temperatures by using eqn (3):

$$K(T) = \alpha(T)/([C_T/n]^{n-1}[1 - \alpha(T)]^n) \quad (3)$$

where n is the number of strands involved in the thermodynamic equilibrium and C_T, the sum of their concentrations. In the case of the hairpin alone in solution, $n = 1$,[42] and in the case of the hairpin/target solution, $n = 2$.[43,44] This equation is only available for non-self-complementary duplexes. A van't Hoff plot of $\ln(K(T))$ *vs.* $1/T$ was generated for both folded hairpin and duplex formation. The slope and intercept of the calculated line yielded the enthalpy (ΔH°) and the entropy (ΔS°), respectively, according to eqn (4):

$$\ln(K(T)) = -(\Delta H^\circ/R)/T + \Delta S^\circ/R \quad (4)$$

where R is the gas constant (1.987 cal K^{-1} mol^{-1}) and T the temperature in Kelvin. The Gibbs free energy at 298 °K (ΔG°_{298}) was calculated according to eqn (5):

$$\Delta G^\circ_{298} = \Delta H^\circ - 298\Delta S^\circ \quad (5)$$

The obtained data represent at least the average of minimum five independent experiments on hairpin and duplex formations. The errors addressed on the thermodynamic data result from the standard deviation of the three experiments. Standard deviation calculated for T_m values are within ±0.9 °C and those of ΔH°, ΔS° and ΔG°_{298} are within ±10%.

Electrochemical measurements

Each ApiT8 biochip was sonicated 5 min in an ethanol–water (50/50) solution and activated with a NaOH solution (0.5 M) by chronoamperometry between −800 and 1200 mV (four times). Electrodes were rinsed with water and dried under argon before use.

Experiments on ApiT8 were performed in a droplet (10 µL) of phosphate buffer (25 mM Na_2HPO_4, 25 mM KH_2PO_4, 250 mM $NaClO_4$, pH = 6.4).

Cyclic voltammetry was performed at a potential range from −300 to + 300 mV. For all measurements, four successive cycles were achieved for signal stabilization and the fourth was kept as data.

Faradaic charge was measured at 80 min after the probe solution deposition on the ApiT8 electrodes (scan rate = 100 mV s^{-1})

ODN probes (10 µL of either 100 µM Fc-ODNs (B, F) or 5 µM Fc-ODN D in 25 mM phosphate, 250 mM $NaClO_4$) were deposited on the biochip gold electrodes and the system was left for stabilization during 80 min. Diagnostic tests were carried out by introducing the target in the droplet. Electrochemical response was followed by CV before and after the target addition (scan rate: 100 mV s^{-1}; potential range: −300/+300 mV); [Fc–ODN] = 100 µM and [target] = 550 µM (5.5 eq.) for the Fc-modified hairpins B and F and [Fc–ODN] = 5 µM and [target] = 27.5 µM (5.5 eq.) for the Fc-modified hairpin D.

Acknowledgements

Our thanks to Professors Olivier Vittori, Didier Leonard and Pierre Lantéri for welcoming us to the "Laboratoire des Sciences Analytiques", Lyon 1 University. We also thank Pr Frédéric Fages from CINaM and Pr Errachid from LSA for helpful discussion on the work. This work was supported by bioMérieux. We are grateful to Bouchra Makrouf from bioMérieux for the provision of the gold electrode microarrays (ApiT8) produced by Nicosofra.

References

1 C. A. Marquette, M. F. Lawrence and L. J. Blum, *Anal. Chem.*, 2006, **78**, 959.
2 A. Tsourkas, M. A. Behlke, Y. Xu and G. Bao, *Anal. Chem.*, 2003, **75**, 3697.
3 S. Tyagi and F. R. Kramer, *Nat. Biotechnol.*, 1996, **14**, 303.
4 R. Wilson and M. K. Johansson, *Chem. Commun.*, 2003, 2710.
5 S. A. E. Marras, S. Tyagi and F. R. Kramer, *Clin. Chim. Acta*, 2006, **363**, 48.
6 M. Culha, D. L. Stokes, G. D. Griffin and T. Vo-Dinh, *Biosens. Bioelectron.*, 2004, **19**, 1007.
7 C. Ma, Z. Tang, K. Wang, W. Tan, J. Li, W. Li, Z. Li, X. Yang, H. Li and L. Liu, *Anal. Biochem.*, 2006, **353**, 141.
8 M. J. Serra, T. J. Axenson and D. H. Turner, *Biochemistry*, 1994, **33**, 14289.
9 G. R. Bishop, J. Ren, B. C. Polander, B. D. Jeanfreau, J. O. Trent and J. B. Chaires, *Biophys. Chem.*, 2007, **126**, 165.
10 G. Bonnet, S. Tyagi, A. J. Libchaber and F. R. Kramer, *Proc. Natl. Acad. Sci. U. S. A.*, 1999, **96**, 6171.
11 M. Szemes and C. D. Schoen, *Anal. Biochem.*, 2003, **315**, 189.
12 G. Leone, H. v. Schijndel, B. v. Gemen, F. R. Kramer and C. D. Schoen, *Nucleic Acids Res.*, 1998, **26**, 2150.
13 S. Tyagi, S. A. E. Marras and F. R. Kramer, *Nat. Biotechnol.*, 2000, **18**, 1191.
14 D.-M. Kong, L. Gu, H.-X. Shen and H.-F. Mi, *Chem. Commun.*, 2002, 854.
15 J. R. Patel, A. A. Bhagwat, G. C. Sanglay and M. B. Solomon, *Food Microbiol.*, 2006, **23**, 39.
16 J. Li, H. Yan, K. Wang, V. Tan and X. Zhou, *Anal. Chem.*, 2007, **79**, 1050.
17 E. Knoll and T. Heyduk, *Anal. Chem.*, 2004, **76**, 1156.
18 B. Bockisch, T. Grunwald, E. Spiliner and R. Bredehorst, *Nucleic Acids Res.*, 2005, **33**, e101.
19 C. Fan, K. W. Plaxco and A. J. Heeger, *Proc. Natl. Acad. Sci. U. S. A.*, 2003, **100**, 9134.
20 C. Fan, K. W. Plaxco and A. J. Heeger, *Trends Biotechnol.*, 2005, **23**, 186.
21 A.-E. Radi, J. L. A. Sanchez, E. Baldrich and C. K. O'Sullivan, *J. Am. Chem. Soc.*, 2006, **128**, 117.
22 Y. Xiao, X. Qu, K. W. Plaxco and A. J. Heeger, *J. Am. Chem. Soc.*, 2007, **129**, 11896.
23 Y. Jin, X. Yao, Q. Liu and J. Li, *Biosens. Bioelectron.*, 2007, **22**, 1126.
24 E. Pavlovic, R. Y. Lai, T. T. Wu, B. S. Fergusson, R. Sun, K. W. Plaxco and H. T. Soh, *Langmuir*, 2008, **24**, 1102.
25 Y. Mao, C. Luo and Q. Ouyang, *Nucleic Acids Res.*, 2003, **31**, e108.
26 A. Sassolas, B. D. Leca-Bouvier and L. J. Blum, *Chem. Rev.*, 2007, **108**, 109.
27 A.-E. Navarro, N. Spinelli, C. Moustrou, C. Chaix, B. Mandrand and H. Brisset, *Nucleic Acids Res.*, 2004, **32**, 5310.
28 A.-E. Navarro, N. Spinelli, C. Chaix, C. Moustrou, B. Mandrand and H. Brisset, *Bioorg. Med. Chem. Lett.*, 2004, **14**, 2439.
29 A.-E. Navarro, F. Fages, C. Moustrou, H. Brisset, N. Spinelli, C. Chaix and B. Mandrand, *Tetrahedron*, 2005, **61**, 3947.
30 H. Brisset, A.-E. Navarro, N. Spinelli, C. Chaix and B. Mandrand, *Biotechnol. J.*, 2006, **1**, 95.
31 G. Chatelain, C. Chaix, H. Brisset, C. Moustrou, F. Fages and B. Mandrand, *Sens. Actuators, B*, 2008, **132**, 439.
32 G. Deglane, S. Abes, T. Michel, P. Prévot, E. Vives, F. Debart, I. Barvik, B. Lebleu and J.-J. Vasseur, *ChemBioChem*, 2006, **7**, 684.
33 D. J. Williams and K. B. Hall, *Biochemistry*, 1996, **35**, 14665.
34 F. Garnier, B. Bouabdallaoui, P. Srivastava, B. Mandrand and C. Chaix, *Sens. Actuators, B*, 2007, **123**, 13.

35 A. J. Bard and L. R. Faulkner, *Electrochemical Methods: Fundamentals and Applications*, John Wiley & Sons Inc., New York, 2nd edn, 2001.
36 C. Farre, N. Spinelli, A. Bouchet, C. Marquette, B. Mandrand, F. Garnier and C. Chaix, *Synth. Met.*, 2007, **157**, 125.
37 X. Luo, T. M.-H. Lee and I. M. Hsing, *Anal. Chem.*, 2008, **80**, 7341.
38 C. R. Cantor, M. M. Warshaw and H. Shapiro, *Biopolymers*, 1970, **9**, 1059.
39 M. J. Cavaluzzi and P. N. Borer, *Nucleic Acids Res.*, 2004, **32**, e13.
40 L. A. Marky and K. J. Breslauer, *Biopolymers*, 1987, **26**, 1601.
41 M. Durand, K. Chevrie, M. Chassignol, N. T. Thuong and J. C. Mauriziot, *Nucleic Acids Res.*, 1990, **18**, 6353.
42 R. N. Hannoush and M. J. Damha, *J. Am. Chem. Soc.*, 2001, **123**, 12368.
43 G. E. Plum, *Current Protocols in Nucleic Acid Chemistry*, John Wiley & Sons, Inc., New York, 2000.
44 N. B. Ramsing, K. Rippe and T. M. Jovin, *Biochemistry*, 1989, **28**, 9528.